DOI: 10.1002/cbic.200700153

Mutational Analysis of the Myxovirescin Biosynthetic Gene Cluster Reveals Novel Insights into the Functional Elaboration of Polyketide Backbones

Vesna Simunovic and Rolf Müller*[a]

*It has been proposed that two acyl carrier proteins (ACPs)—TaB and TaE—and two 3-hydroxy-3-methylglutaryl synthases (HMGSs)—TaC and TaF—could constitute two functional ACP-HMGS pairs (TaB/TaC and TaE/TaF) responsible for the incorporation of acetate and propionate units into the myxovirescin A scaffold, leading to the formation of β-methyl and β-ethyl groups, respectively. It has been suggested that three more proteins—TaX and TaY, which are members of the superfamily of enoyl-CoA hydratases (ECHs), and a variant ketosynthase (KS) TaK—are shared between two ACP-HMGS pairs, to give the complete set of enzymes required to perform the β-alkylations. The β-methyl branch is presumably further hydroxylated (by TaH) and methylated to produce the methoxymethyl group observed in myxovirescin A. To substantiate this hypothesis, a series of gene-deletion mutants were created, and the effects of these mutations on myxovirescin production were examined. As predicted, Δ*taB *and* Δ*taE *ACP mutants revealed similar phenotypes to their associated HMGS mutants Δ*taC *and* Δ*taF, respectively, thus providing direct evidence for the role of TaE/TaF in the formation of the β-ethyl branch and implying a role for TaB/TaC in the formation of the β-methyl group. Production of myxovirescin A was dramatically reduced in a Δ*taK *mutant and abolished in both the* Δ*taX *and the* Δ*taY *mutant backgrounds. Analysis of a* Δ*taH *mutant confirmed the role of the cytochrome P450 TaH in hydroxylation of the β-methyl group. Taken together, these experiments support a model in which the discrete ACPs TaB and TaE are compatible only with their associated HMGSs TaC and TaF, respectively, and function in a substrate-specific manner. Both TaB and TaC are essential for myxovirescin production, and the TaB/TaC pair can rescue antibiotic production in the absence of either TaE or TaF. Finally, the reduced level of myxovirescin production in the* Δ*taE *mutant, relative to the* Δ*taF *strain, suggests an additional function of the TaE ACP.*

Introduction

Polyketides and nonribosomal peptides are structurally diverse classes of secondary metabolites, assembled from carboxylic-CoA esters and amino acids, respectively.[1] They are biosynthesized by specialized protein megacomplexes, which are organized into functional units called modules, each of which accomplishes a specific round of chain extension. These multienzyme systems are known as polyketide synthases (PKS) and nonribosomal peptide synthetases (NRPS), respectively. Typically, each module minimally incorporates three domains: an acyltransferase (AT), which selects specific extension units, a ketosynthase (KS), which catalyses carbon bond formation, and an acyl carrier protein (ACP), to which the growing chain is tethered in thioester linkage. Following condensation, the β-ketoacyl-*S*-ACP intermediate could be further reduced by one of the optional domains (keto reductase (KR), dehydratase (DH), and enoyl reductase (ER)), before being transferred from the ACP to the KS of the next module for another round of chain extension. The biosynthesis thus follows a linear-assembly program directed by the particular combination of catalytic domains present within each module, and the number and order of modules within the PKS. The thioesterase (TE) located within the last module terminates the assembly process by facilitating the release of the fully extended product by hydrolysis or lactonization.

In addition to the genes encoding type I PKSs, the biosynthetic gene clusters responsible for myxovirescin, bacillaene, mupirocin, and several other compounds also include a set of discrete genes named "HMG-cassettes".[2–5] Each HMG-cassette comprises a set of five genes encoding for a 3-hydroxy-3-methylglutaryl-CoA synthase (HMGS), an ACP, a variant KS (in which the active site Cys is mutated to Ser), and two homologues of enoyl-CoA hydratases (ECH)[5] (Figure 1 A). Furthermore, the PKSs responsible for these compounds often belong to the so-called "*trans*-AT" family of type I synthases, which lack integral AT domains, and hence compensate for these activities with *trans*-acting ATs.

[a] *M.S. V. Simunovic, Prof. Dr. R. Müller*
Pharmaceutical Biotechnology, Saarland University
P.O. Box 151150, 66041 Saarbrücken (Germany)
Fax: (+49) 681-302-5473
E-mail: rom@mx.uni-saarland.de

Supporting information for this article is available on the WWW under http://www.chembiochem.org or from the author.

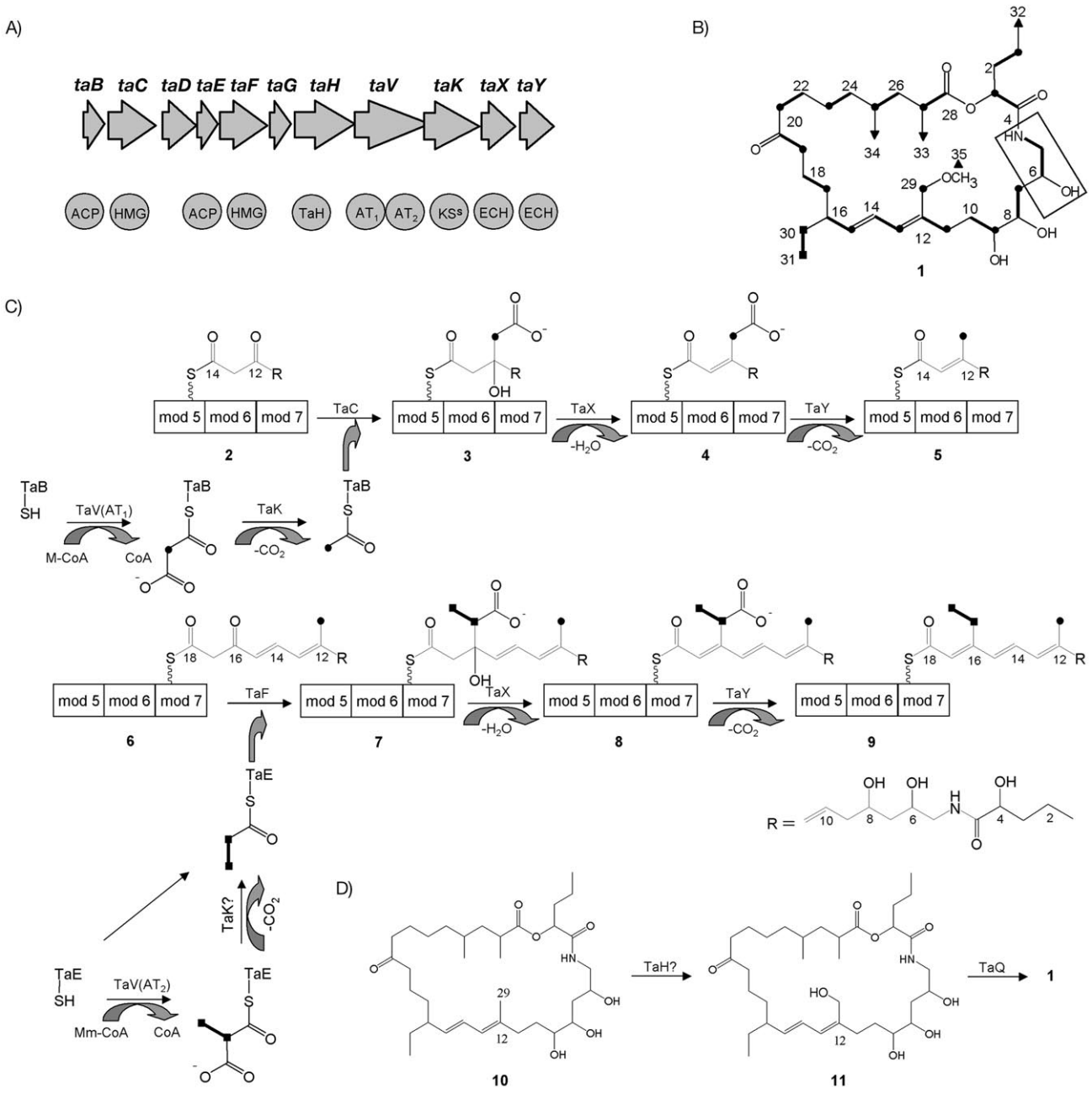

Figure 1. A) 10.9 kb fragment of the myxovirescin A biosynthetic gene cluster encoding for monofunctional enzymes. TaB and TaE are putative ACPs, TaC and TaF are homologues of HMG-CoA synthases, TaK is a variant β-ketoacyl-ACP synthase (KS^{Q}), TaX and TaY are homologues of enoyl-CoA hydratases (ECH), and TaH is a putative cytochrome P450. B) Structure of myxovirescin A (**1**) indicating the biosynthetic origin of its building units.[6] Boxed carbons originate from glycine, circles indicate C2 of acetate, triangles indicate methyl groups derived from methionine, and connected squares show the ethyl group originating from carbons 2 and 3 of succinate. C) A working model of myxovirescin A assembly depicts two rounds of modification reactions leading to the formation of C12 β-methyl and C16 β-ethyl side groups in the myxovirescin scaffold. Two ATs encoded by TaV load malonyl-CoA (M-CoA) and methylmalonyl-CoA (Mm-CoA), respectively, onto their cognate ACPs (TaB and TaE), which become substrates of the decarboxylase TaK. Alternatively, propionyl-CoA could be directly loaded on TaE to give propionyl-*S*-TaE. Condensation of intermediate **2** with acetyl-*S*-TaB and of intermediate **6** with propionyl-*S*-ACP, catalyzed by the HMGSs TaC and TaF, respectively, creates intermediates **3** and **7**. Removal of the carboxylate groups from intermediates **3** and **7** is a two-step process involving dehydration by TaX (resulting in intermediates **4** and **8**), followed by their sequential decarboxylation to yield **5** and **9**. The carbon labeling pattern is described in (B). D) Following the formation of intermediate **9**, five more rounds of polyketide extension encoded by TaO and TaP PKSs and hydroxylation at C9 take place to yield **10**. Hydroxylation of **10** at C29 yields **11**, which becomes the subsequent target of *O*-methyltransferase TaQ, giving myxovirescin A (**1**).

It has been proposed that the gene products of the HMG-cassettes constitute a separate pathway dedicated to the formation of the β-methyl branches in these secondary metabolites. In vitro studies of HMG cassette enzymes from the bacillaene (PksX) pathway have demonstrated their likely in vivo roles in the biosynthesis: the discrete AT charges the ACP with the appropriate substrate (typically malonyl-CoA or methylmalonyl-CoA), the variant KS catalyzes decarboxylation, while the

HMGS acts to couple the resulting acetate or propionate unit to the polyketide backbone (Figure 1C). Finally, the two ECH homologues modify the resulting intermediate further by removing water and the carboxylate group.

In comparison with similar metabolites that display characteristic β-methyl branches, myxovirescin A has a unique β-ethyl branch originating from the C2/C3 part of succinate, via methylmalonate (Figure 1B).[6] It has been speculated that the formation of both β-branches takes place through this newly characterized pathway and requires the two pairs of freestanding ACP and HMGS activities (TaB/TaC and TaE/TaF), respectively (Figure 1A). It has also been proposed that the two HMG-CoA-like synthases TaC and TaF might carry out nucleophilic additions of acetyl-*S*-TaB and propionyl-*S*-TaE onto the C12 and C16 β-keto positions of the β-ketoacyl-*S*-ACP polyketide intermediates **2** and **6**, respectively.[3;7] As the other three enzymes, the variant KS (TaK^S) and the two enoyl-CoA hydratase homologues (TaX and TaY), are encoded only once in the gene cluster, it has been proposed that they might be involved in both rounds of modification reactions (Figure 1C). Following the formation of the C29 methyl carbon connected to C12 and the ethyl group attached to C16, it has been suggested that antibiotic biosynthesis might switch back to the classical polyketide biochemistry to generate the myxovirescin lactone ring (**10**). Hydroxylation of the C29 carbon and its subsequent methylation would then yield the methoxymethyl group present in myxovirescin A (**1**; Figure 1D).

In our previous study, we presented genetic evidence that both HMGSs are required for the biosynthesis of myxovirescin A. Deletion of *taC* caused the loss of **1**; this shows that TaC is indispensable for myxovirescin production. However, TaF was not absolutely required, as its inactivation led to the production of a novel myxovirescin analogue.[7] This new metabolite contained a methyl group in place of the ethyl group at C16, providing direct evidence for the role of TaF in the formation of the ethyl group. Furthermore, production of this novel myxovirescin was not dependent on the primary metabolic HMGS *mvaS*, the only other HMGS homologue identified in the *Myxococcus xanthus* DK1622 genome.[7] Hence, the presence of a novel β-methyl branch in the new myxovirescin analogue (myxovirescin ΔF) was explained by the double action of TaC, which appears to be capable of complementing the function of TaF.[7] To test the remainder of the proposed biosynthetic model, a series of in-frame mutants was created and extracts of the resulting strains were analyzed by high-performance liquid chromatography/mass spectrometry (HPLC-MS) for the production of **1**, its analogues, or possible precursors.

Results

Δ*taB* and Δ*taE* mutants produce phenotypes similar to those observed for their corresponding HMGSs mutants Δ*taC* and Δ*taF*

As suggested by the gene organization in the cluster and the low level of sequence homology between the two discrete ACPs TaB and TaE (33% identity, 51% similarity), TaB and TaE were predicted to interact with their associated HMGS TaC and TaF by forming two functional complexes (TaB/TaC and TaE/TaF; Figure 1A). It was thus hypothesized that each functional ACP/HMGS pair might perform one round of substrate-specific β-alkylation on the C12 and C16 β-keto positions of intermediates **2** and **6** (Figure 1B–C). However, prior to associating with their presumed HMGSs, each ACP would have to be acylated with a specific substrate (TaB with malonate and TaE with methylmalonate), by one of the two ATs present in the cluster, and further decarboxylated by a common decarboxylase TaK (Figure 1C). If the two ACPs and HMGS indeed formed two distinct functional pairs, removal of each ACP from the megacomplex should have yielded the same phenotype as observed for deletions of their presumed HMGSs.[7]

To test these assumptions, both *taB* and *taE* were deleted from the DK1622 genome to yield the *M. xanthus* strains VS1038 (Δ*taB*) and VS1039 (Δ*taE*). HPLC-MS analysis of their mutant extracts revealed the loss of production of **1** in both strains (data not shown). Moreover, the Δ*taE* mutant displayed production of the modified myxovirescin analogue that had previously been isolated from the Δ*taF* HMGS mutant background.[7] This myxovirescin analogue contains a novel C16 β-methyl branch, and was designated myxovirescin ΔF (**12**; Figure 2A). However, since the levels of **12** in the Δ*taE* mutant were reproducibly lower then in the Δ*taF* background, quantitative HPLC-MS analysis was performed to establish its exact concentration. Figure 2A shows that the production of **12** in the Δ*taE* background was ten times lower than in the Δ*taF* strain, thus indicating an additional role for TaE.

TaB and TaK are required for the formation of β-methyl branches

Because the Δ*taF* strain specifically produces analogue **12**, which contains two acetate-derived β-methyl groups (one of which is subsequently modified into a β-methylene), this background was chosen to confirm that TaB/TaC, along with TaK, act in the pathway leading to the formation of **12**. Accordingly, both *taB* and *taK* were deleted from the Δ*taF* mutant, and the effects of the double mutations on the production of **12** were analyzed. As expected, HPLC-MS analysis of the resulting VS1041 (Δ*taBF*) and VS1042 (Δ*taKF*) double mutant extracts indicated the loss of production of **12** (Table 1).

TaK, a variant ketosynthase, is not absolutely required for myxovirescin A production

taK, like many other discretely encoded KS domains found in the HMGS-containing natural product gene clusters, can be distinguished from standard KSs because of its Cys-to-Ser substitution in the active site (KS^S). Biochemical analysis of fatty acid KSs from *E. coli* with the identical mutation have shown the enzymes to be severely deficient in catalyzing condensation, while retaining their decarboxylative functions.[8;9] Recently, PksF of *Bacillis subtilis*, which shows 54% identity and 71% similarity with TaK, has been shown to participate in the pathway dedicated to β-methylation, by catalyzing decarboxylation

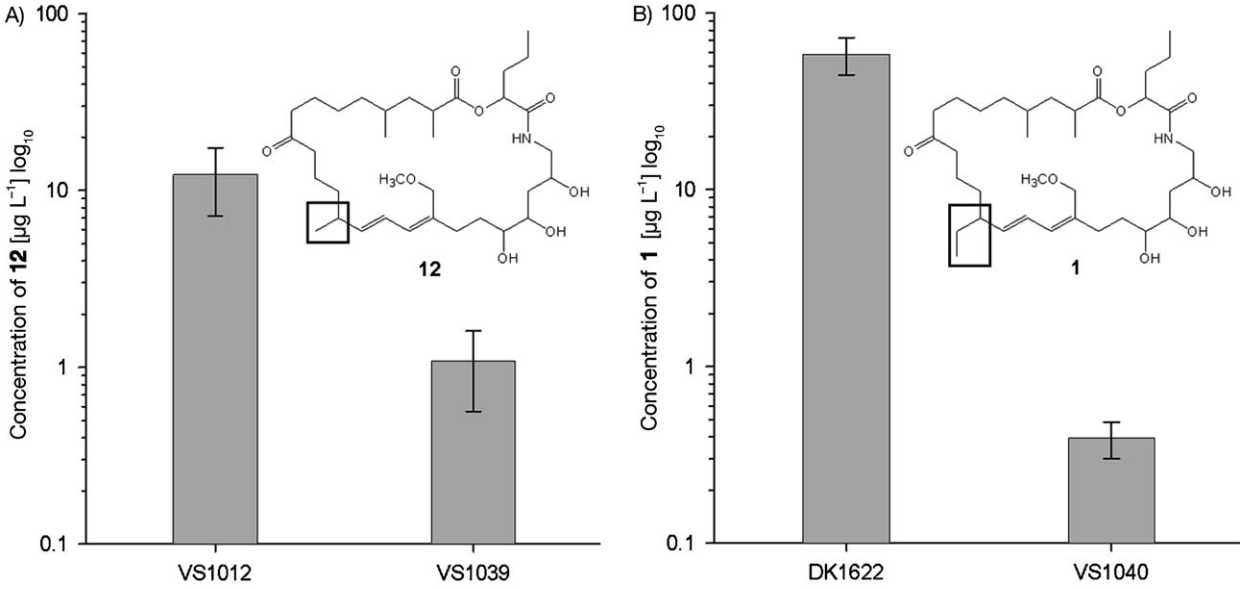

Figure 2. Quantitative HPLC-MS analysis of A) VS1012 (Δ*taF*) and VS1039 (Δ*taE*) and B) DK1622 and VS1040 (Δ*taK*). The error bars represent the standard deviation obtained from five independent experiments. Compounds **1** and **12** were quantified by use of Bruker quantification software by integration of three major $[M+H]^+$ peaks (578.5, 560.5, and 542.5 of **12** and 592.5, 574.5, and 556.5 peaks of **1**).

Table 1. List of *M. xanthus* strains used in this study.

Strain	Genotype	Myxovirescin analogue	Ref.
DK1622	*M. xanthus* wild-type	A (**1**)	[14]
VS1019	pVS59 x DK1622	–	this study
VS1020	pVS60 x DK1622	–	this study
VS1028	pVS71 x DK1622	–	this study
VS1032	pVS83 x DK1622	–	this study
VS1033	pVS82 x DK1622	–	this study
VS1034	pVS82 x VS1012	–	this study
VS1035	pVS81 x DK1622	–	this study
VS1036	pVS81 x VS1012	–	this study
VS1023	Δ*taY*	–	this study
VS1026	Δ*taX*	–	this study
VS1038	Δ*taB*	–	this study
VS1039	Δ*taE*	ΔF (**12**)	this study
VS1012	Δ*taF*	**12**	[7]
VS1040	Δ*taK*	**1**	this study
VS1041	Δ*taBF*	–	this study
VS1042	Δ*taKF*	–	this study
VS1030	Δ*taH*	ΔH (**10**)	this study

of malonyl-*S*-ACP to acetyl-*S*-ACP[5] (compare Figure 1C). Since there is only a single copy of such a mutant KS^S present in the whole DK1622 genome, and two predicted decarboxylation reactions, it has been postulated that TaK acts twice during biosynthesis to cleave carboxyl groups from both malonyl and methylmalonyl-*S*-ACP substrates (Figure 1C). Therefore, removing *taK* from the system would be expected to abolish myxovirescin biosynthesis. In order to verify the involvement of TaK in myxovirescin biosynthesis, *taK* was deleted from the genome and the effect of this mutation on **1** was analyzed. However, contrary to our expectations, production of **1** was still observed in VS1040 (Δ*taK*), although at 120-fold reduced levels relative to the wild-type (Figure 2B).

TaX and TaY, two members of ECH superfamily, are required for myxovirescin A production

Both TaX and TaY show similarity with members of the enoyl-CoA hydratase superfamily. In particular, TaX is more similar to PksH of bacillaene and CurE from the curacin systems, which both catalyze dehydrations (Figure 3A), whereas TaY is more closely related to the decarboxylases PksI and CurF (Figure 3B).[5,10] Based on the sequence homologies with these biochemically characterized enzymes, it was proposed that TaX could dehydrate intermediates **3** and **7**, to yield **4** and **8**, respectively. Further removal of carboxyl groups from **4** and **8** by TaY should yield intermediates **5** and **9**, respectively (Figure 1C). Unfortunately, aside from the observed loss of **1**, HPLC-MS analysis of VS1026 (Δ*taX*) and VS1023 (Δ*taY*) mutant extracts did not reveal the production of new analogues of **1** with additional hydroxyl and carboxyl groups attached to carbons C12/C29 and C16/C31, or hydrolytic release of possible intermediates **3**, **4**, **7**, or **8** (Figure 1B–C).

TaH, a cytochrome P450, hydroxylates the β-methyl group of myxovirescin A

As indicated in Figure 1D, following the assembly of the myxovirescin skeleton, formation of mature myxovirescin A requires three more modification reactions. We have previously shown that the last step in the formation of the methoxymethyl group is catalyzed by the SAM-dependent methyltransferase TaQ (Figure 1B).[3] The two remaining reactions are hydroxylations, which would be expected to target carbons C9 and C29. The three candidates for these two reactions are TaH, assigned as a cytochrome P450 hydroxylase (E value $= 3 \times 10^{-51}$), and two putative oxygenases TaN and TaJ.[3]

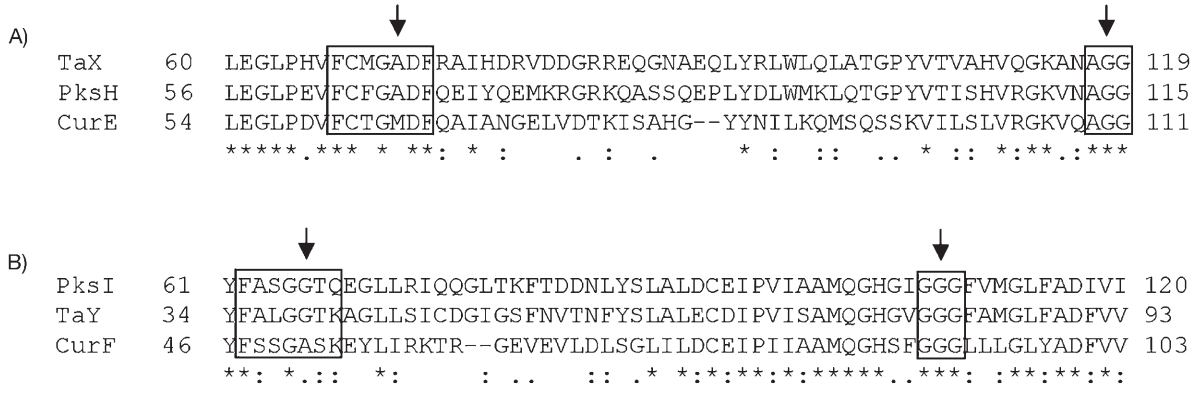

Figure 3. ClustalW alignments of TaX and TaY with members of the ECH superfamily from bacillaene (PksX) and curacin (Cur) systems. PksH (CAB13587) and CurE (AAT70100) have been demonstrated to function as dehydratases, while PksI (CAB13588) and CurF (AAT70101) act as decarboxylases.[5,10] The accession numbers are indicated in parentheses. Arrows indicate amino acids that stabilize the thioester carbonyl group by hydrogen bonding through their peptidic NH groups.

To determine the molecular target of TaH, *taH* was deleted in frame from the DK1622 chromosome, resulting in strain VS1030. Comparative analysis of mass chromatograms of extracts of wild-type DK1622 (Figure 4A, left) and VS1030 (Figure 4A, right; *m/z* 590–625) revealed an approximately 1 min delay in the retention time of myxovirescins in strain VS1030 relative to the wild type. The UV absorption maxima at 239 nm showed the same trend (Figure 4B). In particular, strain VS1030 did not produce **1** ($[M+H]^+ = 624$), but a novel myxovirescin analogue of $[M+H]^+ = 594$. A tandem MS fragmentation of $[M+H]^+ = 594$ confirmed that this new compound, named myxovirescin ΔH, does not fragment to give a $[M+H-32]^+$ ion, which is characteristic of the fragmentation of **1** (Figure 4C, bottom). All the subsequent fragmentations, however, followed a pattern identical to the one observed with the reference compound (compare Figure 4C). Furthermore, the high-resolution mass spectrum (HRMS) of myxovirescin ΔH ($[M+H]^+ = 594.4358$) is in good agreement with the molecular formula $C_{34}H_{60}O_7N^+$ (calculated *m/z* $[M+H]^+ = 594.4364$, $\Delta m/z = -1.08$ ppm, see the Supporting Information), consistent with the loss of a methoxy group relative to **1**.

To confirm whether the largest fragment ion resulting from the fragmentation of **1** is indeed a product of the elimination of the C29 methoxy group (neutral loss, $\Delta m/z = 32$ units), **1** was subjected to MS-MS fragmentation and the HRMS of the largest molecular ion ($[592]^+$) was determined. The calculated HRMS of 592.4208 was in agreement with the experimentally determined mass, and corresponds to the molecular formula $C_{34}H_{58}O_7N^+$, reflecting the loss of methanol (CH_3OH) relative to **1** (Supporting Information). As there is only one methoxy group present in **1**, myxovirescin ΔH was assigned structure **10** (Figure 1D). Interestingly, the production of **10** in VS1030 was equal to the levels of **1** measured in the reference strain (Figure 4B).

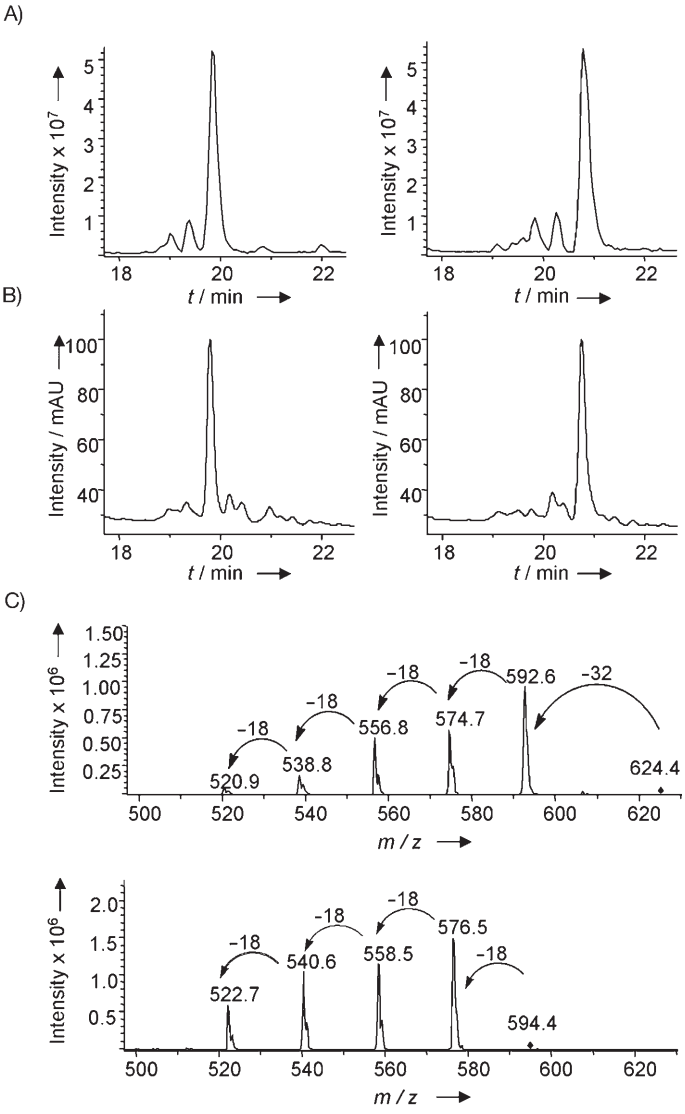

Figure 4. Analysis of the cytochrome P450 mutant strain VS1030 (Δ*taH*). A) Mass ion chromatograms in the 590–625 range from the *M. xanthus* DK1622 (left) and VS1030 (Δ*taH*) strains (right). B) $UV_{239\,nm}$ absorption measured in DK1622 (left) and VS1030 (right). C) Tandem MS fragmentation patterns of myxovirescin A ($[M+H]^+ = 624$) (top) and the novel myxovirescin ΔH ($[M+H]^+ = 594$) (bottom).

Discussion

Our model for myxovirescin A (**1**) assembly proposes that the two ACP/HMGS pairs are β-branch-specific, whereas TaK, TaX,

and TaY are shared between the two pathways (Figure 1C). Indeed, in our previous study we showed that removal of TaC halts myxovirescin biosynthesis whereas the loss of TaF leads to the production of a new myxovirescin with two methyl groups at the C12 and C16 positions (the methyl group at C12 being further elaborated into the methoxymethyl functionality). In this study we have demonstrated that deletions of their proposed accompanying ACPs—TaB and TaE—yield similar phenotypes (Table 1 and Figure 2A). These results provide direct evidence that each ACP has a cognate HMGS with which it forms a functional pair (e.g., TaB with TaC and TaE with TaF). The ACPs are thus not functionally exchangeable during biosynthesis; for example, TaB does not function in combination with TaF, or TaE with TaC. Furthermore, these results demonstrate the functional roles of the two enzyme pairs: the TaB/TaC pair directs formation of the methyl group, while TaE/TaF directs formation of the ethyl group.

Another important conclusion arising from this genetic study is that the functions of the two ACP/HMGS enzyme pairs are not mutually complementary. Our results suggest that TaB/TaC can rescue myxovirescin production in the absence of either TaE or TaF, most likely by performing two rounds of acetate delivery (TaB) and acetate condensation (TaC) with intermediates **2** and **6** to manufacture myxovirescin ΔF (**12**). However, the reverse situation cannot occur, as the TaE/TaF enzyme duo cannot substitute for TaB/TaC. Therefore, both TaB and TaC are essential for antibiotic assembly. In addition, the ability of TaB/TaC to complement TaE/TaF implies a level of flexibility of the TaB/TaC pair in docking with module 7 of Ta-1, as well as the flexibility of module 8 in processing the intermediate with the shorter side chain. However, the molecular determinants for these protein–protein interactions are not known at present.

Given the expectation that deletions of *taB* and *taE* should mimic deletions of their partner HMGSs phenotypically, it was surprising to measure a tenfold drop in the production of **12** in the Δ*taE* strain relative to the Δ*taF* background (Figure 2A). This result demonstrates that the loss of TaE is even more incapacitating to the megasynthetase than the loss of the condensing enzyme TaF, and points to an additional and as yet unknown function of TaE in biosynthesis. The observed functional differences between TaB and TaE are also consistent with their low sequence identity. Indeed, given the central role of ACPs in PKS and fatty acid biosynthesis, as well as in the pathway leading to β-methyl group formation, it is plausible that the divergence of the ACPs was required to ensure the correct spatial implementation of two different substrates in the myxovirescin polyketide scaffold.

It was proposed that TaK, unlike the two ACPs, acts twice during biosynthesis, by decarboxylating both malonyl-*S*-TaB and methylmalonyl-*S*-TaE intermediates (Figure 1C). Unexpectedly, production of myxovirescin A continued in the Δ*taK* background, albeit at a 120-fold reduced level. However, the production of **12** was completely abolished in the Δ*taKF* background. The genome search for possible homologues of TaK did not identify another monofunctional KS exhibiting a similar mutation. Taken together, these results indicate the role of TaK in the formation of the β-methyl branch and suggest either that a different enzyme decarboxylates methylmalonyl-*S*-TaE, or that the corresponding *trans*-AT loads propionyl-CoA directly onto TaE ACP. Alternatively, the residual amount of myxovirescin A observed in the Δ*taK* background could be generated through availability of the low amount of spontaneously decarboxylated malonyl-*S*-ACP and methylmalonyl-*S*-ACP.

Finally, analysis of the cytochrome P450 mutant has provided the last clue towards understanding of the biosynthesis of the methoxymethyl group (Figure 1D and Figure 4). The formation of **10** in the strain VS1030 fully confirms our hypothesis regarding the two-step conversion of the methyl into the methoxymethyl group. In contrast to the severe impact of other mutations on myxovirescin production (Table 1),[3;7] production of **10** in Δ*taH* was equal to the production of **1** in DK1622 (Figure 4B). From this result we conclude that the conversion of **10** to **1** takes place following the formation of the lactone ring.

An emerging body of evidence combining both in vitro and in vivo observations on the bacillaene and myxovirescin systems demonstrates the evolutionary divergence of primary and secondary metabolic (SM) HMGSs. These differences include the demonstrated use of ACP- instead of CoA-activated substrates.[5] Furthermore, SM HMGSs show wide promiscuity toward different substrates. For example, certain HMGS are likely to accept propionyl-*S*-ACP in addition to acetyl-*S*-ACP as a substrate, and to perform nucleophilic additions on β-ketoacyl-*S*-ACP intermediates of different chain lengths. For example, PksG is catalytically active with acetoacetyl-*S*-ACP even though its natural substrate is predicted to be 15 carbons long.[4;5] Similarly, our results suggest that TaF acts on a substrate with a C18 chain length.[7] As no structure of a SM HMGS has yet been solved, it is to be hoped that future high-resolution structural information on members of this newly recognized family of condensing enzymes will be able to provide deeper insights into their flexibility toward heterogeneous substrates.

In contrast to the HMG-like synthases, which have preserved the overall reaction mechanism, members of the ECH superfamily are well known for their mechanistic diversity and catalyze various reactions ranging from dehalogenation, (de)hydration, decarboxylation, formation/cleavage of carbon-carbon bonds, hydrolysis of thioesters, etc.[11] Despite the overall differences in their reaction mechanisms, ECH family members share a partial reaction mechanism that enables stabilization of enoyl-CoA anion intermediates within an oxyanion hole (residues outlined in two boxes; Figure 3). However, consistent with the different overall reactions that they catalyze, the active site residues within the superfamily vary.

Two homologues of this superfamily have been found to be conserved across several biosynthetic gene clusters.[2;5;12;13] In vitro characterizations of two pairs of ECHs from the bacillaene and curacin systems, and the very recent characterization of TaX and TaY (C. Calderone, C. T. Walsh et al., personal communication) have demonstrated their functions as dehydratases and decarboxylases, respectively.[5;10] At this point we cannot ascertain whether the observed loss of myxovirescin production in Δ*taX* and Δ*taY* backgrounds is a result of the rejection

of the proposed intermediates **3**, **4**, **7**, or **8** by the assembly line, or by the requirement of the two enzymes for megasynthetase turnover, or both.

Conclusions

The mutagenic analysis of eight discrete genes encoded in the myxovirescin gene cluster constitutes the first comprehensive in vivo study geared towards the elucidation of the biosynthetic pathway leading to the formation and tailoring of β-branches in one secondary metabolite. In addition to the elucidation of functional roles of certain genes, our results present evidence for the plasticity of myxovirescin megasynthase. However, several aspects of the biosynthesis remain to be elucidated, including the nature of protein–protein interactions between β-modifying enzymes and the PKS multienzyme. Nonetheless, the relative ease of manipulating discretely encoded activities, in contrast to the giant polyketide synthases, coupled with the observed broad substrate specificity of HMGS and ECH homologues, suggests that HMG toolboxes and their accessory enzymes might be successfully exploited in future attempts to generate new, "β-modified" bioactive compounds.

Experimental Section

Creation of deletion mutants: The general cloning strategy used for the construction of vectors intended for creation of in-frame deletions of Δ*taB*, Δ*taE*, Δ*taH*, and Δ*taK* is demonstrated here with the deletion of *taK*. To delete *taK*, the chromosomal region including *taK* and approximately 600 bp upstream and downsteam from it was amplified with the aid of K1 and K2 primers (see the Supporting Information) and Phusion polymerase (New England Biolabs). The resulting 2276 bp PCR product carrying *Bam*HI and *Xba*I overhangs was gel purified (Macherey und Nagel), modified with A overhangs, and cloned in pCR2.1®-TOPO vector, yielding plasmid pVS72. Plasmid pVS72 was amplified in the second PCR reaction by use of primers K3 and K4, designed to be in-frame with *taK*, and Phusion polymerase. Following amplification, the PCR reaction was treated with *Dpn*I enzyme to eliminate the template DNA. The 5 kb PCR product was gel-purified, treated with T4 kinase and T4 ligase, and transformed into *E. coli* DH10B. The new plasmid, pVS76, lacking the *taK* gene but containing the 600 bp upstream and downstream of the gene, was submitted for sequencing. Finally, the approximately 1200 bp insert was subcloned from pVS76 into *Bam*HI and *Xba*I sites of vector pSWU41 to create plasmid pVS79, which was used for electroporation in *M. xanthus* DK1622. The cloning strategy used to generate plasmids for Δ*taX* and Δ*taY* mutantions, as well as the creation of in-frame deletion mutants, was carried out as described in ref. [3]. To create Δ*taEF* and Δ*taKF* double mutants, plasmids pVS81 and pVS79, respectively, were electroporated, and later excised, from the chromosome of VS1012 (Δ*taF* background). Sequences of all primers are provided in the Supporting Information, and the list of generated plasmids is given in Table 2.

Growth conditions: Myxovirescin production was assayed in MD-1 medium that consisted of casitone (0.3%), $CaCl_2 \cdot 2H_2O$ (0.07%), and $MgSO_4 \cdot 7H_2O$ (0.2%); vitamin B12 (5×10^{-4} μg L^{-1}) was added after cooling, and the system was analyzed for myxovirescin production as reported previously.[3]

Table 2. Plasmids generated in this study.

Plasmid	Plasmid description
pVS44	627 bp fragment obtained by amplification with TaX1 and TaX2 primer pair; cloned in pTOPO
pVS45	617 bp fragment obtained by amplification with TaX3 and TaX4 primer pair; cloned in pTOPO
pVS46	578 bp fragment obtained by amplification with TaY1 and TaY2 primer pair; cloned in pTOPO
pVS47	550 bp fragment obtained by amplification with TaY3 and TaY4 primer pair; cloned in pTOPO
pVS59	Inserts from pVS46 and pVS47 cloned in *Xba*I and *Spe*I sites of pSWU41
pVS60	Inserts from pVS44 and pVS45 cloned in *Xba*I and *Spe*I sites of pSWU41
pVS66b	2560 bp fragment amplified with H1/H2 primer pair containing *taH* plus ca. 600 bp on either side of the gene; cloned in pTOPO vector
pVS68	2560 bp fragment amplified with H1/H2 primers and cloned in *Xba*I and *Spe*I sites of pSWU41
pVS71	Derivative of pVS68 obtained by amplification with H3/H4 primer pair; the construct lacks 1422 bp of *taH*
pVS72	2276 bp fragment containing *taK* plus ca. 600 bp on both sides of the gene amplified with K1/K2 primer pair and cloned in pTOPO vector
pVS73	1484 bp fragment containing *taB* and ca. 600 bp on both sides of the gene amplified with B2/B3 primer pair and cloned in pTOPO vector
pVS77	1425 bp fragment containing *taE* and ca. 600 bp on both sides of the gene amplified with E2/E3 primer pair and cloned in pTOPO vector
pVS78	Derivative of pVS72 lacking 1179 bp of *taK* (Δ*taK*). Obtained by amplification of pVS72 with K3/K4 primer pair.
pVS79	Derivative of pVS73 lacking 240 bp of *taB* (Δ*taB*). Obtained by amplification of pVS73 with B1/B4 primer pair.
pVS80	Derivative of pVS77 lacking 201 bp of *taE* (Δ*taE*). Obtained by amplification of pVS77 with E1/E4 primer pair.
pVS81	1097 bp fragment from pVS78 subcloned in *BamH*I/*Xba*I sites of pSWU41
pVS82	1244 fragment from pVS79 subcloned in *BamH*I/*Xba*I sites of pSWU41
pVS83	1224 bp fragment from pVS80 subcloned in *BamH*I/*Xba*I sites of pSWU41

HPLC-MS analysis and quantification of 1 and myxovirescin ΔF: HPLC-MS analysis and quantitative HPLC-MS analysis were carried out as described.[3] Myxovirescin ΔF was quantified by integrating three major peaks at *m/z* 576.5, 558.5, and 540.6.

High-resolution mass spectral analysis (HRMS): Determination of HRMS of myxovirescin ΔH and its fragment ions was carried out by ESI-FT/Orbitrap mass spectrometry. Measurements were performed with an UPLC-coupled LTQ Orbitrap instrument (Thermo Finnigan, Bremen, Germany) in positive ionization mode with a resolution setting of $R = 60\,000$. External calibration in the *m/z* range 195–2000 was performed with "LTQ Calibration solution" containing caffeine, MRFA (Met-Arg-Phe-Ala tetrapeptide), and the "Ultramark 1621" reference mixture. Calculation of the putative molecular formula from the accurate mass spectra of target compounds was performed with the Xcalibur 2.0 software suite.

Acknowledgements

The authors would like to thank Dr. K. J. Weissman for helpful comments in the preparation of this manuscript and D. Krug for

help with quantitative HPLC-MS and for performing the Orbi-Trap measurements. This study was funded by the Deutsche Forschungsgemeinschaft (DFG) and the Bundesministerium für Bildung und Forschung (BMBF).

Keywords: antibiotics · cytochromes · methylation · *Myxococcus xanthus* · polyketides

[1] M. A. Fischbach, C. T. Walsh, *Chem. Rev.* **2006**, *106*, 3468 – 3496.
[2] A. K. El-Sayed, J. Hothersall, S. M. Cooper, E. Stephens, T. J. Simpson, C. M. Thomas, *Chem. Biol.* **2003**, *10*, 419 – 430.
[3] V. Simunovic, J. Zapp, S. Rachid, D. Krug, P. Meiser, R. Müller, *ChemBioChem* **2006**, *7*, 1206 – 1220.
[4] R. A. Butcher, F. C. Schroeder, M. A. Fischbach, P. D. Straight, R. Kolter, C. T. Walsh, J. Clardy, *Proc. Natl. Acad. Sci. USA* **2007**, *104*, 1506 – 1509.
[5] C. T. Calderone, W. E. Kowtoniuk, N. L. Kelleher, C. T. Walsh, P. C. Dorrestein, *Proc. Natl. Acad. Sci. USA* **2006**, *103*, 8977 – 8982.
[6] W. Trowitzsch-Kienast, K. Schober, V. Wray, K. Gerth, H. Reichenbach, G. Höfle, *Liebigs Ann. Chem.* **1989**, 345 – 355.
[7] V. Simunovic, R. Müller, *ChemBioChem* **2007**, *8*, 497 – 500.
[8] C. Davies, R. J. Heath, S. W. White, C. O. Rock, *Structure* **2000**, *8*, 185 – 195.
[9] K. A. McGuire, M. Siggaard-Andersen, M. G. Bangera, J. G. Olsen, P. von Wettstein-Knowles, *Biochemistry* **2001**, *40*, 9836 – 9845.
[10] L. Gu, J. Jia, H. Liu, K. Hakansson, W. H. Gerwick, D. H. Sherman, *J. Am. Chem. Soc.* **2006**, *128*, 9014 – 9015.
[11] H. M. Holden, M. M. Benning, T. Haller, J. A. Gerlt, *Acc. Chem. Res.* **2001**, *34*, 145 – 157.
[12] J. Piel, G. P. Wen, M. Platzer, D. Q. Hui, *ChemBioChem* **2004**, *5*, 93 – 98.
[13] D. J. Edwards, B. L. Marquez, L. M. Nogle, K. McPhail, D. E. Goeger, M. A. Roberts, W. H. Gerwick, *Chem. Biol.* **2004**, *11*, 817 – 833.
[14] H. Chen, I. M. Keseler, L. J. Shimkets, *J. Bacteriol.* **1990**, *172*, 4206 – 4213.

Received: March 27, 2007
Published online on June 21, 2007

